hydrogen

MDPI

Article

Mitigating Hydrogen Risks in Light-Water Nuclear Reactors: A CFD Simulation of the Distribution and Concentration

Joseph Amponsah [1] and Archibong Archibong-Eso [2,*]

[1] Department of Mechanical Engineering, Iowa State University of Science and Technology, 1801 S Lincoln Way, Ames, IA 50011, USA; josephamponsah069@gmail.com
[2] Department of Mechanical Engineering, University of Birmingham, Dubai Campus, Dubai P.O. Box 341799, United Arab Emirates
* Correspondence: a.e.archibong@bham.ac.uk

Abstract: During severe accidents in light-water nuclear reactors, the release of hydrogen poses significant risks to the integrity of the containment and the surrounding infrastructure. To address this, passive autocatalytic re-combiners (PARs) have been adopted in several countries. However, it remains challenging to eliminate the production of flammable combinations and the potential for local flame explosions, even with PARs installed. Understanding the distribution and concentration of generated hydrogen, particularly in 100% fuel-clad coolant reactions, is therefore crucial. In this study, numerical investigations using ANSYS CFX, a commercially available code, are conducted to analyze the hydrogen generation and distribution in a 1000 MWe nuclear power plant. The results show the effectiveness of PARs through a comparative evaluation of reactors with PARs and without PARs installed. The simulated scenario involved the release of hydrogen from the reactor pressure vessel, resulting in a reduction in the maximum hydrogen concentration released from 17.85% in the containment model without PARs to 9.72% in the containment model with PARs installed after 22,000 s. These findings highlight the importance of understanding and controlling the hydrogen distribution in light-water nuclear reactors during severe accidents. This study is useful in informing the mitigation risks strategy for hydrogen release in light-water nuclear reactors.

Keywords: mitigating hydrogen risks; light-water nuclear reactors; CFD simulation; hydrogen leakages; nuclear power plants

Citation: Amponsah, J.; Archibong-Eso, A. Mitigating Hydrogen Risks in Light-Water Nuclear Reactors: A CFD Simulation of the Distribution and Concentration. *Hydrogen* **2023**, *4*, 709–725. https://doi.org/10.3390/hydrogen4040045

Academic Editors: Vladimir Molkov, Zhang-Hui Lu and Sergio Alberto Obregón Alfaro

Received: 21 May 2023
Revised: 16 August 2023
Accepted: 14 September 2023
Published: 22 September 2023

1. Introduction

Power generation through nuclear plants is one of the cleanest and most efficient electricity generation technologies from conventional energy sources. Nevertheless, public skepticism persists due to the devastating consequences (to the environment, critical infrastructure, and, more importantly, human lives) recorded during rare but severe accidents (SAs) that have occurred in nuclear power plants (NPPs). Of these SAs, three stand out: the 1979 accident on Three Mile Island in the United States; the 1986 accident in the Chornobyl plant in the Soviet Union (present-day Ukraine Republic); and, more recently, the 2011 accident in Fukushima, Japan. Researchers have leveraged advances in computational capabilities by using enhanced computational algorithms to study SAs through numerical simulations and Probabilistic Level-2 Safety Assessments [1]. Further research investigations on SAs were performed after two core meltdown accidents: a severe accident at the Chernobyl RBMK (water-cooled channel-type reactors with graphite as a moderator) on 26 April 1986, and an SA on Three Mile Island on 28 March 1979. During nuclear accidents, reactor fuels are susceptible to overheating, and when this occurs, the zirconium cladding of the fuel rods may react chemically with steam to generate hydrogen. Furthermore, if the generated hydrogen diffuses from the reactor to the containment, it may mix with air to form a flammable and/or explosive mixture depending on the hydrogen concentration and the temperature of the fuel claddings. As a safeguard, passive autocatalytic recombiners

(PARs) are used to remove hydrogen from the containment during accidents, thereby preventing explosions. Typically, in the event of severe accidents, hydrogen production can reach several hundreds of kilograms in an hour, while the most efficient PARs can only remove hydrogen at the rate of 4 kg/hr. This has led to the use of multiple PARs in nuclear plants. An understanding of the flow patterns (the spatial arrangements and distributions of hydrogen gas as it flows through the containment module), hydrogen diffusion (movement of hydrogen molecules from a high-concentration to a low-concentration region), and concentration (volume fraction) when discharged during an accident is critical in designing devices, such as PARs. Furthermore, developing effective mitigation and safety strategies for NPPs can benefit from this insight.

CFD has become an increasingly important tool in nuclear safety analysis and design optimization. Recent studies have demonstrated the use of CFD simulations in a variety of nuclear applications. One such application is the prediction of natural circulation flow during severe accidents in reactor coolant systems [2]. The authors used CFD to study the natural circulation flow in a reactor coolant system during a severe accident. The results showed that the flow pattern and velocity were affected by changes in the coolant temperature and system pressure. The turbulent flow and heat transfer of gas mixtures in circular tubes have also been investigated using CFD [3]. The authors conducted a numerical investigation of the turbulent flow and heat transfer of a helium–xenon gas mixture in a circular tube. The study demonstrated that CFD could provide accurate and reliable predictions of fluid flow and heat transfer in complex geometries and for non-Newtonian fluids. In addition, CFD has been used to study single-phase flows in nuclear engineering applications using both Unsteady Reynolds Average Navier–Stokes (URANS) and Large Eddy Simulation (LES) approaches [4]. The authors reviewed the use of URANS and LES approaches for turbulent incompressible single-phase flows in nuclear engineering applications. They discussed the advantages and limitations of each approach and concluded that LES had the potential to provide more accurate and reliable predictions of turbulent flows in nuclear systems. By providing accurate and reliable predictions of fluid flow and heat transfer in nuclear systems, CFD can help improve the safety and efficiency of nuclear power plants.

While substantial work has been conducted in recent years on severe accidents in NPPs, several aspects remain unexplored due to the challenges, such as funding, the complexities of setting up lab-scale facilities for NPP-related research, etc. In 2004, the European Commission (EU) ruled that it was critical to strengthen national efforts to optimize the usage of existing knowledge and experimental facilities to address unresolved concerns about the security of present and future NPPs [5,6]. This culminated in the founding of the Severe Accident Research NETwork of Excellence (SARNET), funded by the EU under the 6th Framework Programme (FP6), which brings together 51 organizations to leverage their expertise in solving challenges in NPPs [7,8]. Significantly, SARNET identified SAs as one of the most important issues in the NPP sector that has remained largely unaddressed. The Fukushima catastrophe demonstrated that SAs can occur despite preventative actions taken by NPP operatives, resulting in severe damage to the reactor core, complete core meltdown, and serious economic and health costs if radioactive products are discharged into the atmosphere. In NPPs, severe accidents are accidents that compromise safety systems at levels that are much higher than envisaged. Often, they involve initial core damage, exceeding the regulatory fuel limit conditions (such as a temperature of 1473 K (1200 °C) in the fuel claddings). These accidents often result from heating issues with the NPP's coolant pump, preventing the core's residual power from being evacuated effectively, as well as several failures caused by equipment and/or human error, including an inability to follow safety precautions [9].

Several complex phenomena arise during SAs depending on the circumstances surrounding the event and on the plant operatives' actions. The critical physical events that may occur during SAs are shown in Figure 1, along with a few of the associated safety

devices. The reactor is submerged in water during normal operations but loses the water in a Loss of Coolant Accident (LOCA), resulting in core damage.

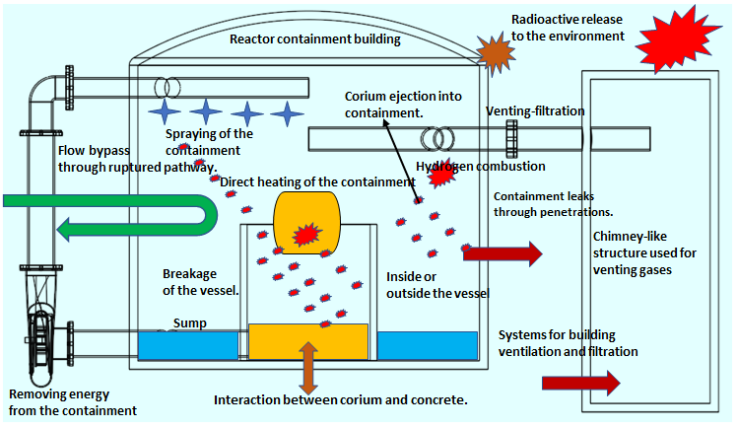

Figure 1. Main physical phenomena during a severe accident.

The oxidation of the zircaloy fuel cladding generate considerable amounts of hydrogen and heat energy [9]. In addition, the low melting-point levels are achieved due to the interactions between the combustion and its cladding. These interactions cause the migration of melting substances, also known as "corium", to the nucleus where volatile fission products are emitted first, followed by the less flammable ones. Within the core, a corium pool eventually forms and progresses toward the vessel's lower head, and when it encounters any remaining water, it vaporizes, thereby fragmenting the corium. A backup water supply to the Reactor Coolant System (RCS) or secondary cooling system may be provided during core degradation. Flooding a degraded core is a sophisticated operation that, in certain situations, may postpone or halt the progression of the catastrophe [10]. Reflooding, on the other hand, may result in an increase in hydrogen production and the emission of more nuclear byproducts.

Influenced by factors in the RCS, the corium melts, debris accumulates in the lower head of the container, and the vessel can explode due to heat erosion, creep, or mechanical failure. When a vessel ruptures because of internal pressure buildup, a part of the expelled corium breaks and may be distributed throughout the confinement. This might result in a pressure spike, considerable thermal radiation with the ambient environment, degradation of the metallic components of the lateral compartment, and, in some of these instances, coordinated combustion of the hydrogen contained within the confinement. This phenomenon is termed "direct containment heating". The WWER 440/213 nuclear power station was benchmarked as part of the PHARE project using CFD models to simulate a specific catastrophic accident scenario that comprised hydrogen emission and distribution [11]. These investigations show CFD algorithm capabilities in simulating the movement of gas throughout the whole enclosure for untreated and PAR-mitigated instances. The outcomes demonstrate the viability of using both specialist (GASFLOW) and general commercial algorithms (ANSYS Fluent, CFX) for these types of simulations. Void of established assumptions outside the code's base setup, CFD codes still demonstrated the ability to predict stratified flow in the study's enclosure.

The development of GASFLOW-MPI was motivated by the need to simulate large-scale problems in the nuclear safety analysis, which require significant computational resources.

Recently, the Boiling Water Reactor (BWR) Mark III at Corrente's nuclear power station was evaluated for the performance of installed PARs as part of the European nuclear facilities' stress tests [12]. To reduce the likelihood of rising hydrogen emissions and accumulation after a catastrophic accident, the authors created a technique for calculating the quantity and location of PARs. The primary sources of mass and energy-restrictive situations were initially obtained using a lumped parameter code (MAAP4). Subsequently, hy-

drogen distribution in the study's confined environment was examined using the GOTHIC 3D containment code [13]. To optimize the PARs' enhanced mitigation mechanism effectiveness, the authors investigated the size and placement of the PARs. The authors concluded that when mitigation using PARs was implemented, there was a considerable decrease in hydrogen accumulation and, hence, in the danger of combustion.

The Chornobyl, Fukushima, and TMI-2 nuclear power plant tragedies demonstrate how critical it is to maintain containment integrity to minimize fission product leakage into the environment. While incorporating Passive Autocatalytic Recombiners (PARs) into a Pressurized Water Reactor (PWR) is one approach to decreasing hydrogen explosion concerns, the PARs' positions are crucial since this not only affects the hydrogen concentration and flow pattern in the region, but also the PARs' efficiency. To minimize numerical errors in the modeling, practice guidelines are developed [14]. These guidelines, together with a detailed simulation setup, may be necessary for studies that focus on the determination of the correct placement of PARs due to taking into consideration factors, such as hydrogen release location and rate, hydrogen distribution, geometry, operational limits, etc. [7,15]. Models and validated codes have made great progress in the design and analysis of hydrogen mitigation measures in nuclear power plants, as well as in developing strategies for accident management [10]. However, from the literature reviewed, it is noted that studies whose emphasis is on hydrogen distribution in the containment model with PARs installed are sparse. Researchers either focus on PARs or on the containment model and not necessarily on both components. Consequently, the objective of this study is to demonstrate high-fidelity CFD capabilities in studying hydrogen distributions in containment models with and without PARs installed.

2. Materials and Methods

2.1. Grids and Parameters for Calculations

Containment Model and Grid Systems

Figure 2a,b shows the CAD geometry and computational mesh grids of the containment structure used in this study. The geometry was designed using commercially available CAD software, Solidworks while meshing, which was used to discretize the geometry into computational domains with the aid of Autodesk® Inventor. Commercially available and widely used CFD code ANSYS® CFX was used for the simulation studies. To reduce numerical errors, a grid independence study was conducted. The mesh grids with hexahedral cells with 1.6 million nodes, tetrahedral cells with 1.9 million nodes, and 1.3 million nodes were used. The containment model had a height of about 70 m and a diameter of 38 m. The compartments are normally located below the operation deck at a height of about 22 m. Some main components of the loops were arranged symmetrically in the model. The containment deck had a height of 5.5 m supporting the major heavy components in the containment, including steam generators. There were some parts in the containment that were designed mainly for the safety injection tanks. The relief valve was connected to the reactor cavity in the model sector, which also reached the wall of the containment and had a length of 24 m. The size of the mesh in the containment was also adjusted according to each location of the containment structures so that the model or geometry could be defined with a meshing system with a heavy cost of computation.

The simulation is based on the boiling water reactors in Figure 2a,b. In this research, the BWR used demineralized water as a coolant and neutron moderator. Heat was produced by nuclear fission in the reactor core, and this caused the cooling water to boil, producing steam. The impact of the mesh resolution and near-wall treatment was investigated using four distinct computational meshes (a two-layer model or wall functions). The four meshes were built in a similar manner. The properties of the four meshes are displayed in the table below. A composite mesh of tetrahedral and hexahedral cells composed the fluid regions, and structured tetrahedral mesh cells filled the vessel's basal area. Structured and unstructured hexahedral cells composed the annulus, cylinder, and dome regions. To resolve the flow and physical phenomena more thoroughly at the wall, the mesh was

refined toward the walls and solid structures. Similarly, the small inlet and injection jet were modified to clearly capture the flow at and above the inlets. Table 1 provides a list of the properties of the four meshes. The usual cell sizes in the y + = 1 mesh are 0.2 mm close to the walls and 70 to 38 mm in the bulk. The typical cell sizes in the normal, granular, and fine mesh are 71 mm close to the walls and 70 and 38 mm in the bulk, respectively.

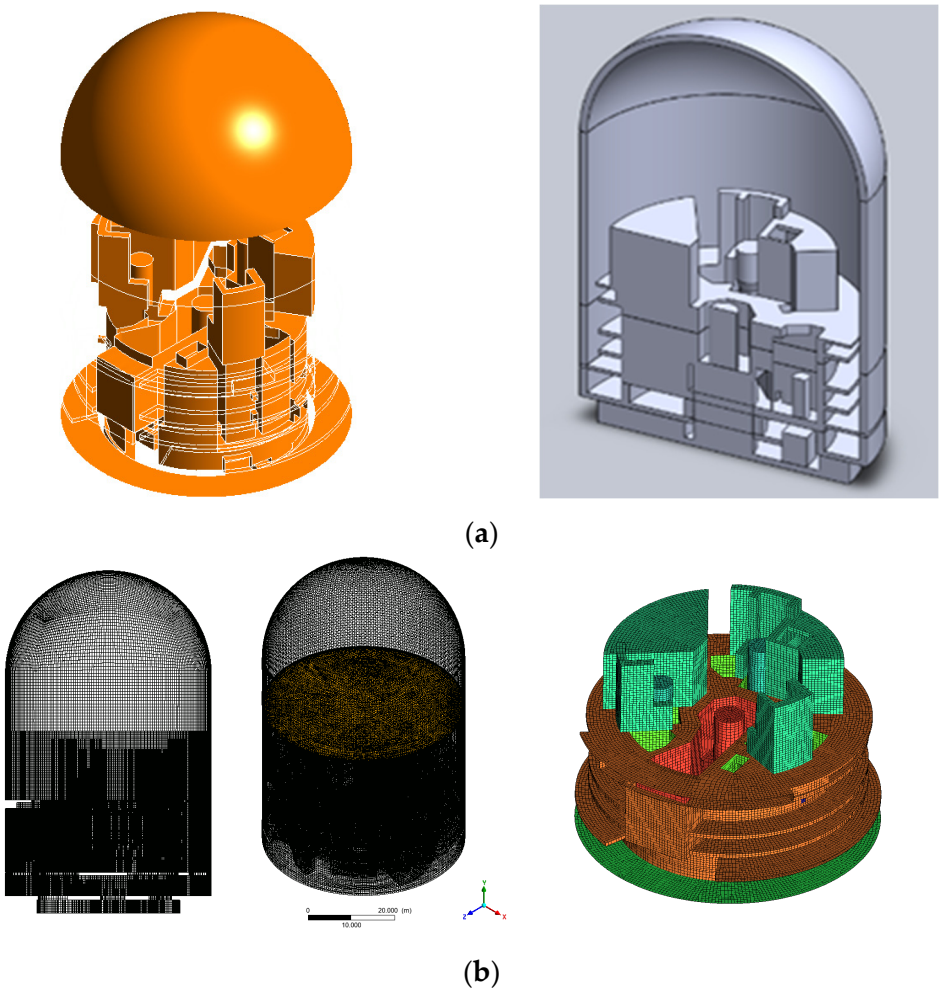

Figure 2. (**a**) Three-dimensional containment model. (**b**) Mesh of the 3D containment model.

Table 1. The properties of the meshes.

Mesh Level	Number of Cells	Velocity at r = 0.02 m (m/s)	Velocity at r = 0.04 m (m/s)	Velocity at r = 0.06 m (m/s)	Velocity at r = 0.08 m (m/s)
Coarse	961,437	0.024	0.044	0.062	0.08
Medium	100,000	0.027	0.048	0.067	0.085
Fine	1,400,000	0.028	0.05	0.07	0.088
Very Fine	1,600,000	0.029	0.051	0.071	0.089

To remove hydrogen during a severe accident, 39 PARs were installed in the NPP containment [16,17]. The system was designed in such a way that the spray system in the containment operated in two different modes: the recirculation spraying mode and the direct mode, dependent mostly on the geometrical construction. Pressure is dependent

mostly on the geometrical construction. When such a strain in the containment reaches 3.6 bar, then the direct spray mode should start [16].

The graph depicted in Figure 3 displays the data presented in Table 1. In the direct spray mode, the sprayed water comes directly from the refueling tank. In this case, the nozzle outlet of the temperature starts from 15 to 20 degrees. After 40 min, the refueling tank, which contains water, is also used. Then, the recirculation mode is activated. Within the recirculation mode, water is transferred from the water sump installed within the containment.

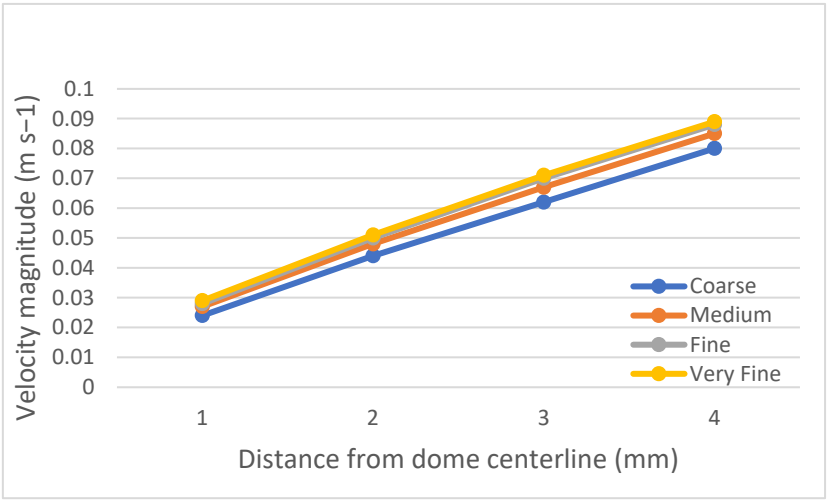

Figure 3. Grid independence study of different mesh distributions.

2.2. Numerical Modeling and Governing Equations

2.2.1. Turbulence Models

Generally, the standard Reynolds-averaged Navier–Stokes (RANS) and Large Eddy Simulation (LES) models with full buoyancy effects and default turbulent constants were utilized for the CFD analyses in this paper. The appropriate turbulence closure models, such as the k-epsilon or k-omega models, are commonly used due to their efficiency and accuracy in predicting the overall flow field in nuclear power plants [18].

2.2.2. Standard $k-\epsilon$ Turbulence Model (LES)

The governing equations for Large Eddy Simulations (LESs) are the filtered Navier–Stokes equations, which are given by:

$$\partial(\rho k)\partial t + \nabla\cdot(\rho k V) = \nabla\cdot\left[\left(\mu + \frac{\mu}{\sigma k}\right)\nabla k\right] + Gk + Gb - \rho\epsilon \quad (1)$$

$$\partial(\rho\epsilon)\partial t + \nabla\cdot(\rho\epsilon V) = \nabla\cdot\left[\left(\mu + \frac{\mu}{\sigma\epsilon}\right)\nabla\epsilon\right] + C1\epsilon k(Gk + C3\epsilon Gb) - C2\epsilon\rho\epsilon 2k \quad (2)$$

where Gb is the generation of the turbulence kinetic energy due to buoyancy. Gk is the source term of the turbulent kinetic energy induced by the mean velocity gradient. $C1\epsilon$, $C2\epsilon$, and $C3\epsilon$ are constants. σk and $\sigma\epsilon$ are the turbulent Prandtl numbers for k and ϵ, respectively.

2.2.3. RANS $k-\epsilon$ Model

In RANS, the equations governing the mean flow are solved, with the effects of the turbulent fluctuations modeled using turbulence models. The equations solved in RANS models are the Reynolds-averaged Navier–Stokes equations, which are given by:

$$\frac{\partial(\rho u_i)}{\partial t} + \frac{\partial\left(o u_{iu}^{i} j\right)}{\partial x_j} = -\frac{\partial p}{\partial x_i} + \frac{\partial(\tau, i)}{\partial x_2} + fi \quad (3)$$

where ρ is the fluid density, u_i is the mean velocity component in the i-th direction, p is the pressure, $\tau_{i,j}$, is the Reynolds stress tensor, and fi is the body force component in the i-th direction. The Reynolds stress tensor is a measure of the correlation between turbulent velocity fluctuations, and it is modeled using turbulence models.

2.2.4. Governing Equations

The flow regime is governed by mass and energy conservation equations for all flows and energy conservation in the containment model. This is involved with heat transfer or compressible fluid [16].

The continuity equation can be written as:

$$\frac{\partial \rho}{\partial t} + \nabla \cdot (\rho \mathrm{u}) = 0 \tag{4}$$

where ρ is the density of the fluid, t is time, u is the fluid velocity, and ∇ is the divergence operator. The continuity equation is a fundamental equation in fluid dynamics that expresses the conservation of mass for a fluid. In the context of the numerical simulation of hydrogen diffusion during a severe accident in a nuclear power plant, the continuity equation can be used to model the transport of hydrogen in the reactor containment building [19].

2.2.5. Energy Equation

The energy equation can be written as:

$$C_p \frac{\partial \rho}{\partial t} + \nabla \cdot \left(C_p p T\right) = k \nabla^2 T + Q \tag{5}$$

where ρ is the density of the fluid, C_p is the specific heat capacity of the fluid at a constant pressure, T is the temperature, t is time, u is the fluid velocity, k is the thermal conductivity of the fluid, ∇ is the gradient operator, and Q is the volumetric heat source.

2.2.6. Dome Temperature and Pressure Monitoring

To monitor the flow conditions of the dome utilized in this study, a preliminary investigation was conducted. Figure 4a,b show a plot of the temperature as a function of time, and pressure as a function of time. Both plots show a steep increase in the temperature and pressure from the start of the simulation, with the temperature increasing from about 308 to 327 K and the pressure from 101–114 Pa in about 7 s in both cases. Practically, this occurred at the initial stage of the release of the hydrogen, and it was expected that the temperature and pressure within the dome would increase; this therefore provides some evidence for the viability of the initial setup. A detailed validation for this study is shown in the section that follows.

Within the first 1400 s, 370 kg of hydrogen was released into both case 1 and 2 containments (with and without PARs, respectively), and at 4930 s, the hydrogen concentration reached its peak rate of production due to the enhancement of the zirconium reaction or a steam reaction after a core support failure. The pressure in the NPP containment reached its threshold value at 55 s, and the direct spray began [20]. In these case studies, the release of hydrogen was divided into two periods. The initial period lasted from 1500 to 6500 s. The overall rate of hydrogen volume concentration in the containment reached 10%; however, flammable clouds rarely appeared. Due to the PAR, the hydrogen concentration was reduced to less than 10% before the second hydrogen release period started. However, the release of hydrogen between 1200 and 1450 s can lead to extremely high hydrogen levels. Gas stratification can be observed in Figure 5 in both models with and without PARs.

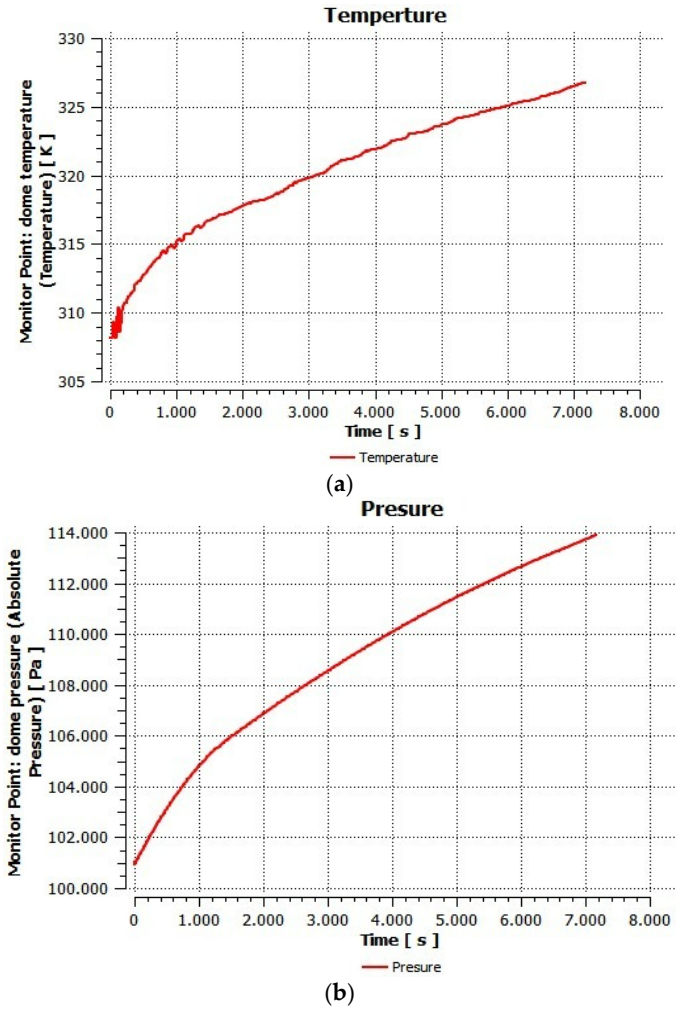

Figure 4. (**a**) Dome temperature as a function of time; (**b**) dome pressure as a function of time.

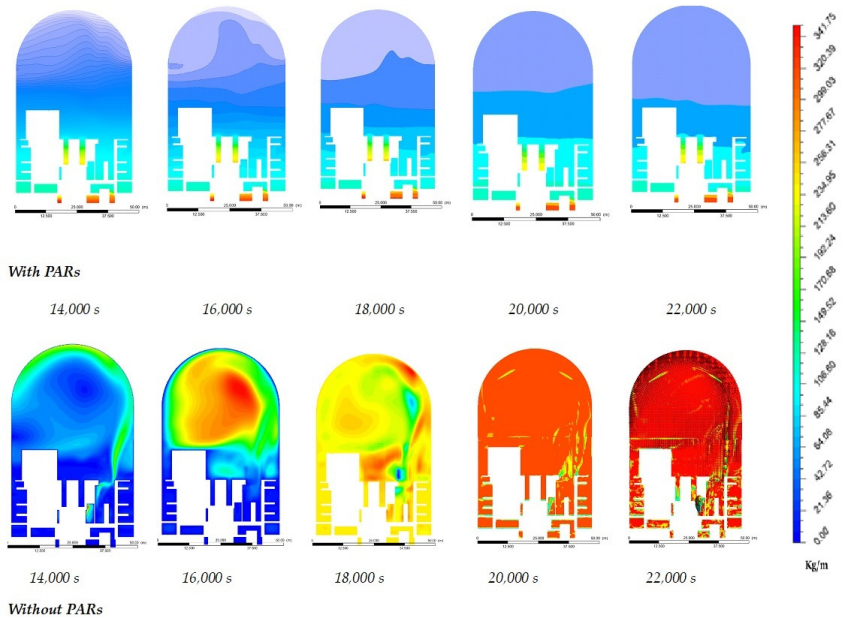

Figure 5. Comparison of hydrogen distributed during the test with and without PARs as a function of time.

To validate and verify the current results, we compare the hydrogen distribution in the current study with and without PARs to two other studies using MAAP, GASFLOW, and COM3D. Hydrogen release clouds in the containment are wrapped by saturated steam-rich clouds for most of the time, providing an inertial atmosphere for the hydrogen and preventing the combustion of hydrogen from occurring too early. The hydrogen release cloud in case 1 has a larger size relative to case 2. Compared to both cases, the concentration of low steam in spray cases [21,22] are significant, which may affect the diffusion and dispersion of the hydrogen release clouds in the containment during a severe accident in a nuclear power plant. Table 2 presents the distribution of hydrogen during different outcomes.

Table 2. Hydrogen concentration distributions for containments with and without PARs.

	Ambient Initial Pressure (bar)	Delta Pressure (bar)	Final Pressure (bar)	Mass (kg)	Initial Volume (m^3)	Compressed Volume (m^3)	Hydrogen
With Recombiner	101,325	10,911	112,236	89.19	49,162	44,382.73	9.72%
Without Recombiner	101,325	22,017	123,342	278.66	49,162	40,386.40	17.85%

3. Results

3.1. Numerical Results

The numerical results show that the simulated severe accident scenario involved a containment vessel with a total volume of 49,162 cubic meters and an initial hydrogen mass of 9.27 kg with PARs installed. Hydrogen was released from the bottom of the reactor pressure vessel. The simulation used a time step of 0.01 s and resulted in a maximum temperature in the containment vessel of approximately 1573 Kelvin. The maximum hydrogen concentration achieved in the containment vessel was approximately 13.5% by volume and occurred after around 16,000 s. The hydrogen plume traveled up to approximately 13 m. The combustion of hydrogen caused a peak overpressure of approximately 0.26 bar for a duration of up to 0.25 s. The peak rate of the pressure increase was approximately 1.7 bar/s and the duration of the pressure increase was up to 0.4 s. These results provide an insight into the behavior of hydrogen during severe accidents in nuclear power plants and can be used to improve safety measures.

3.2. Gas Behavior and Hydrogen Explosion Risk

The manufacturing plans were investigated [3] and measurements were made to corroborate that the built reactor was true to the plans. The containment model was created with CAD and exported as a mesh file into Ansys CFX, from the studies conducted by [23]. From the results of MAAP, at 200 s, the reactor vessel failed and that was quickly followed by an increase in hydrogen production for the model without the installation of PARs, thus resulting in 1614 kg as its final output. A constant production of hydrogen can be seen for the model with PARs installed, resulting in 438 kg as the mass for the hydrogen output. Certain activities were designed to decrease the mass of hydrogen trapped within the confinement, not to alter the hydrogen's flammability limit condition. Once the hydrogen was released into the confinement, its mass within the confinement may be reduced by releasing it. The deflagration of hydrogen was proportional to the mass available; therefore, containment venting was a useful tool for mitigating hydrogen explosion. Studies have shown that venting does not affect hydrogen content [10]. However, this is necessary since the lumped approach is intended [24]. When the whole containment system is viewed as a single node and the vent is triggered, the concentration naturally maintains a consistent value, since the same species is eliminated from the same cell. If, on the other hand, the confinement is shown in three dimensions and ventilation occurs only via a tiny window

(pipe) in the model, venting alters the hydrogen concentration in the various rooms due to the non-homogeneous concentration inside the containment.

During normal operations, the flow within the PAR enclosure undergoes a warming effect and a reduction in viscosity due to the interaction between hydrogen and oxygen in the catalytic zone. This creates a high-speed hot gas that exits the PAR, while the jetting action promotes the mixing of the gas within the container, which is simulated using the standard k-ε turbulence model (with Gb), the SST k-ω turbulence model with Gb, and the SST k-ω turbulence model without a buoyancy effect source term (Gb). In the event of an accident, significant amounts of hydrogen may be released into the containment atmosphere, creating flammable mixtures. The convective flow, consumption, and injection of hydrogen cause the concentration of H2 to vary periodically thereafter. The hydrogen distributed in the containments with and without PARs is presented in Figure 6 at different time intervals.

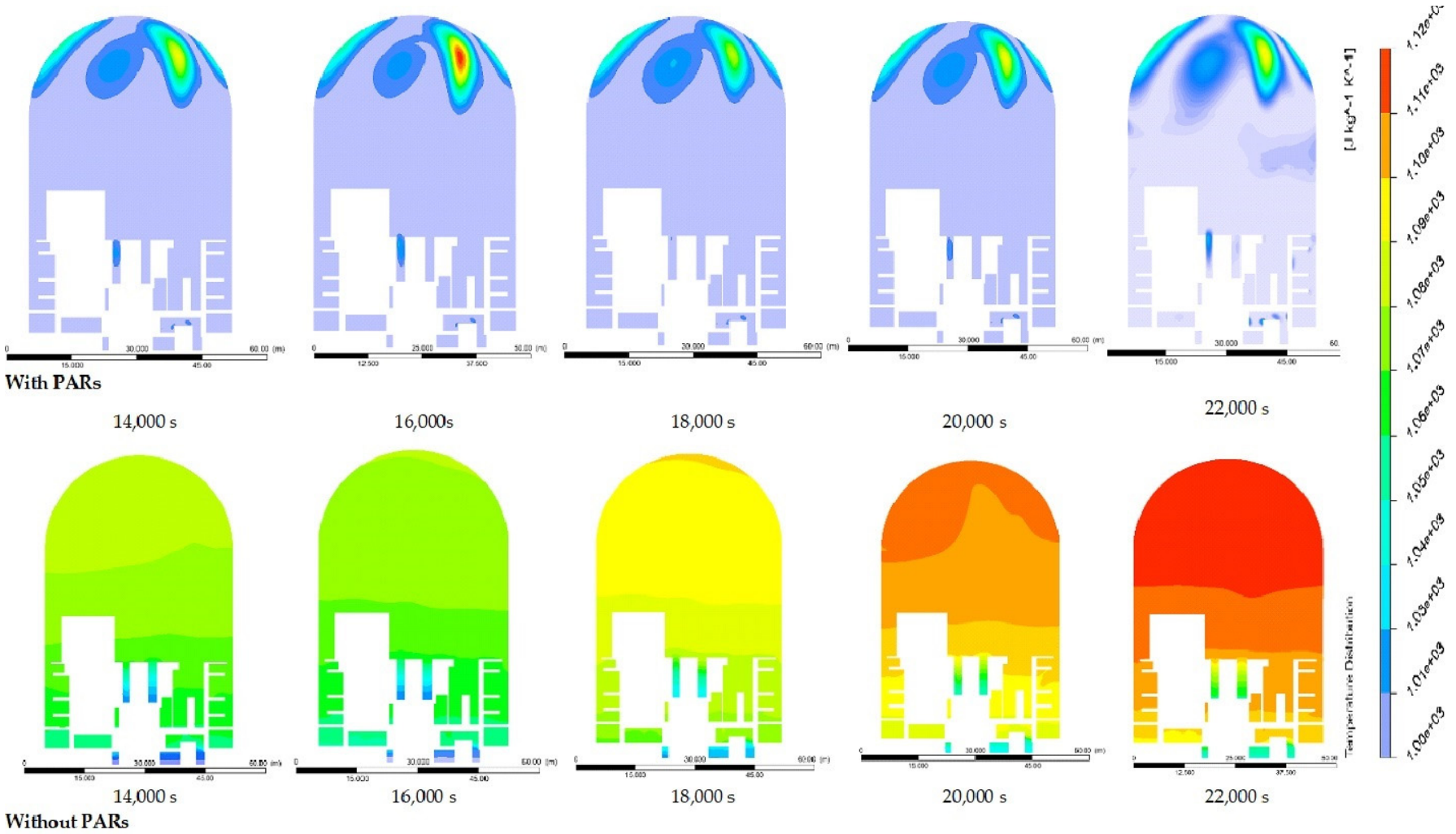

Figure 6. Comparison of temperature distributed during the tests for containments with and without PARs as a function of time.

The contoured charts demonstrate how the PAR works. As the unsteady flow develops, it is possible to witness hydrogen depletion in the PAR near the catalyzed area, as well as the creation of a hydrogen cloud underneath and in front of the PAR. Figure 7 presents snapshots of hydrogen mass flow concentration distributions within containment systems, showcasing scenarios both with (on the right) and without (on the left) Passive Autocatalytic Recombiners (PARs). This is consistent with the experimental findings that indicate some hydrogen stratification in the vessel beginning at 960 s for the HR-2 exam and at 1140 s for the HR-5 assessment [25]. The behavior of hydrogen in a closed vessel equipped with passive autocatalytic recombiners under unsteady flow conditions was investigated in the study. The authors observed that as the unsteady flow developed, hydrogen depletion occurred in the PAR near the catalyzed area, and a hydrogen cloud was created underneath and in front of the PAR. These observations are consistent with the results obtained from the contoured charts that demonstrate how the PAR works. Additionally, hydrogen stratification in the vessel began at 960 s for the HR-2 experiment and at 1140 s for the HR-5 experiment. The CFD temperature was found to be 1573 K, while the hydrogen concentration ranged from 9.72% to 17.85%. They noted that the stratification was caused by the flow separation in the vessel, which led to the accumulation of hydrogen in certain areas of the vessel. In Figure 8, pressure distributions in containment models with and without PARs are depicted as a function of time. This phenomenon can lead to the formation of flammable mixtures, which can pose a safety hazard. The use of PARs can help mitigate this risk by catalytically recombining any hydrogen that may be present in the vessel, thereby preventing the formation of flammable mixtures. Figure 9 illustrates a time-dependent comparison of velocity streamlines within containment systems, contrasting cases with and without Passive Autocatalytic Recombiners (PARs).

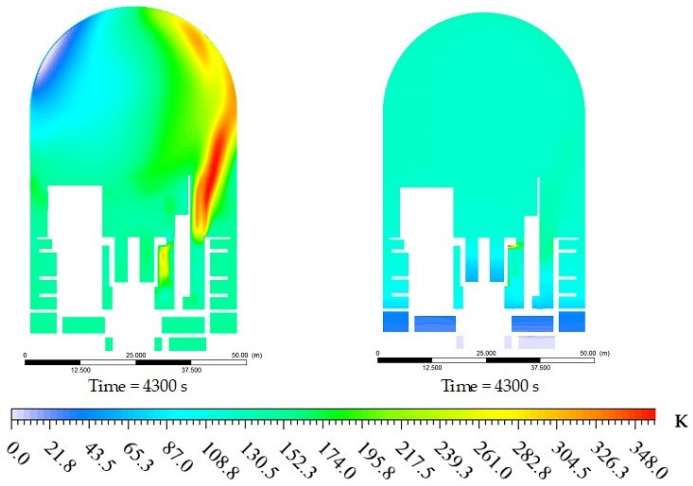

Figure 7. Snapshots of mass flow concentrations of hydrogen distributed in the containments with (**right**) and without (**left**) PARs.

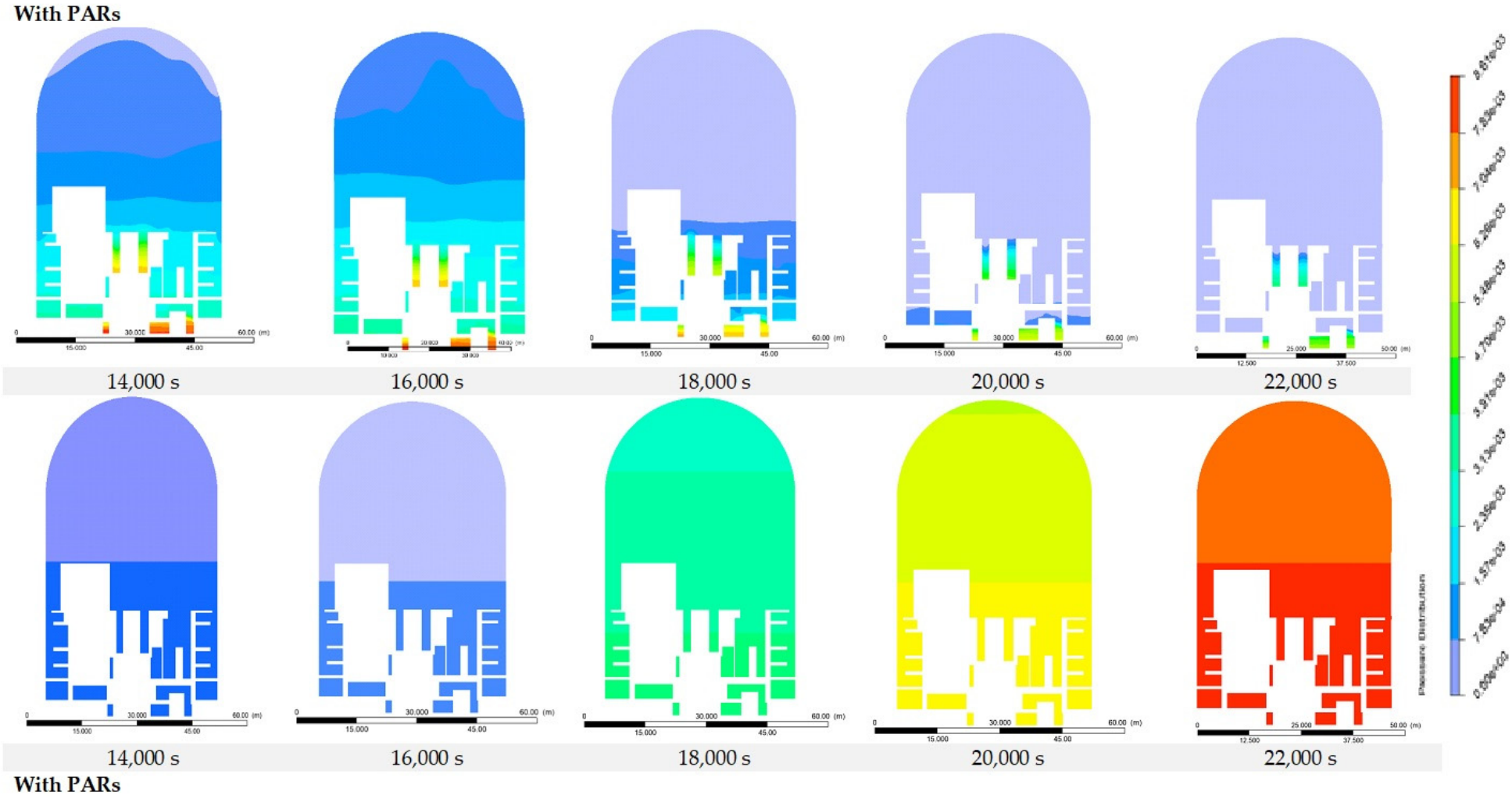

Figure 8. Pressure distributions in containment models with and without PARs as a function of time.

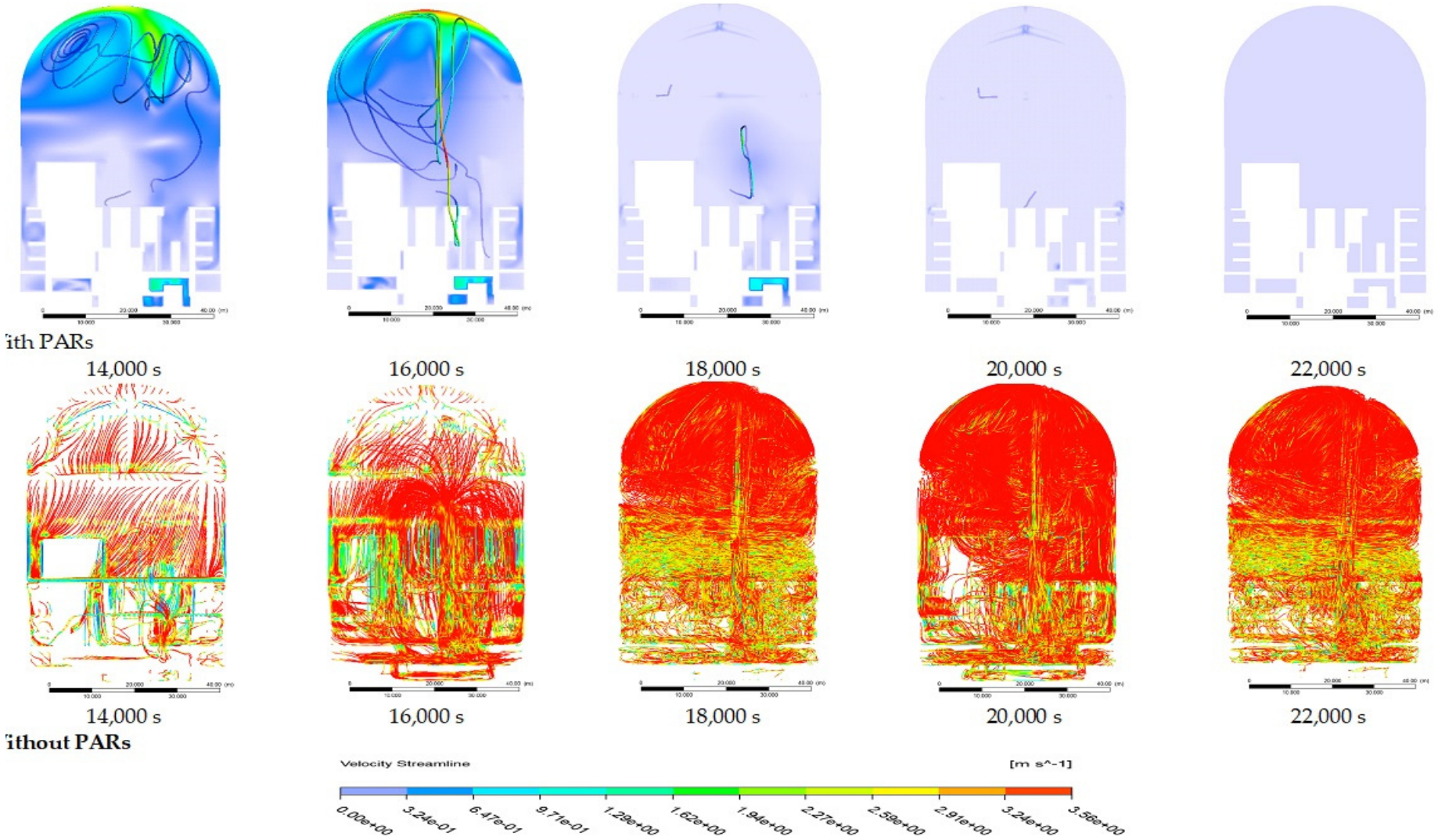

Figure 9. Comparison of velocity streamlines in containments with and without PARs as a function of time.

3.3. Detailed Comparison of the Results

Figure 10 shows the hydrogen concentration in parts per (kg) as a function of time for three different studies: KWU, MAAP/GASFLOW, and CFD. All three datasets show an increasing trend in the hydrogen concentration, which is expected as hydrogen builds up in the system over time. The KWU data start at 5 kg of hydrogen and reach the highest concentration of 52 kg of hydrogen at 22,000 s. It has the steepest increase over time compared to the other two datasets. The MAAP/GASFLOW data start slightly lower at 5 kg of hydrogen and end at 48 kg of hydrogen after 22,000 s. It shows a steady, slightly less steep increase compared to KWU. The CFD results start at 5 kg of hydrogen, which is between KWU's and MAAP/GASFLOW's starting points. It ends at 50 kg of hydrogen, which is also in between the two other final concentrations. Its increase over time is more gradual than KWU, but steeper than MAAP/GASFLOW. The KWU data show the highest concentrations and steepest increase over time. CFD starts and ends between KWU and MAAP/GAS FLOW, with a slope present in between. MAAP/GASFLOW show the lowest starting point, ending point, and most gradual increase in the hydrogen concentrations. The differences demonstrate slightly different hydrogen buildup behaviors between the 3 models/cases, as shown in Figure 10, with KWU predicting faster accumulation times than CFD, and CFD predicting a faster buildup than MAAP/GASFLOW.

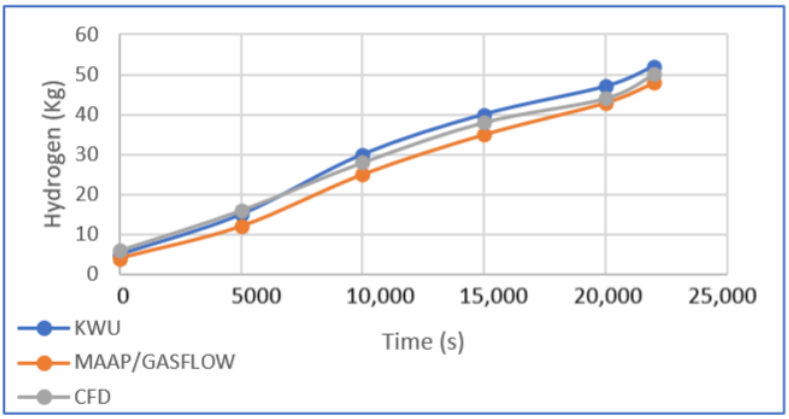

Figure 10. Comparison of CFD, MAAP, and GASFLOW.

4. Conclusions

This study demonstrated the use of Computational Fluid Dynamic (CFD) simulations to analyze the hydrogen distribution and concentration in a pressurized water reactor containment with and without PARs. The CFD code ANSYS CFX was utilized to simulate a severe accident scenario involving hydrogen release from the reactor pressure vessel into the containment. The results show that in the case without PARs, the hydrogen concentration reaches a maximum of 17.85% by volume. With PARs installed, the maximum hydrogen concentration was reduced to 9.72% by volume. This highlights the effectiveness of PARs in limiting hydrogen accumulation. The CFD simulations provided an insight into the temperature and pressure increases within the containment due to hydrogen combustion. The rate of the pressure increase reached approximately 1.7 bar/s. By comparing cases with and without PARs, the CFD study demonstrated the importance of PARs in mitigating the risks of hydrogen deflagration during severe accidents. The results enhance our understanding of hydrogen behavior and distribution within reactor containments. Additional work should involve modeling different hydrogen release scenarios, PAR configurations, and containment geometries. This research demonstrated the capabilities of high-fidelity CFDs in evaluating hydrogen distribution and concentration values within nuclear reactor containments. The study provided valuable data to aid in the design and optimization of passive autocatalytic recombiners and hydrogen risk mitigation systems.

Author Contributions: Conceptualization, J.A.; methodology, J.A. and A.A.-E.; software, J.A.; validation, J.A.; formal analysis, J.A.; investigation, J.A.; resources, A.A.-E.; writing—original draft, J.A.; writing—review and editing, A.A.-E.; supervision, A.A.-E. All authors have read and agreed to the published version of the manuscript.

Funding: This research received no external funding.

Data Availability Statement: Data produced in this study are contained within the article.

Acknowledgments: A.A.-E is grateful to the IT team at the Dubai Campus of the University of Birmingham, especially Philip Keirl, Liam Garey, and Zak Ali who provided excellent support by minimizing the downtime due to hardware malfunctions and ensuring software availability. J.A and A.A.-E are grateful for the support received from the Cape Coast Technical University and the University of Birmingham, respectively.

Conflicts of Interest: The authors declare no conflict of interest.

Abbreviations

NPP	Nuclear Power Plant
PWR	Pressurized Water Reactor
TMI-2	Three Mile Island 2
SA	Severe Accident
LOCA	Loss of Coolant Accident
CFDs	Computational Fluid Dynamics
MCCI	Molten Core–Concrete Interaction
SARNET2	Severe Accident Research Network of Excellence 2
IRSN	Institute for Radiological Protection and Nuclear Safety
RCS	Reactor Coolant System
WWER	Water–Water Energetic Reactor
BWR	Boiling Water Reactor
MAAP4	Modular Accident Analysis Program
RBMK	Reactor Bolshoy Moshchnosty Kanalny

References

1. Micaelli, J.-C.; Haste, T.; Van Dorsselaere, J.-P.; Bonnet, J.-M.; Meyer, L.; Beraha, D.; Annunziato, A.; Chaumont, B.; Adroguer, B.; Sehgal, R.; et al. SARNET: A European Cooperative Effort on LWR Severe Accident Research. *Rev. Générale Nucléaire* **2006**, *1*, 128–135. [CrossRef]
2. Al-Khawaja, A.; Park, H. Numerical study of natural circulation flow in reactor coolant system during a severe accident. *Ann. Nucl. Energy* **2014**, *67*, 290–297.
3. Qin, H.; Fang, Y.; Wang, C.; Tian, W.; Qiu, S.; Su, G.; Deng, J. Numerical investigation on heat transfer characteristics of helium-xenon gas mixture. *Int. J. Energy Res.* **2021**, *45*, 11745–11758. [CrossRef]
4. Benhamadouche, S. On the use of (U)RANS and LES approaches for turbulent incompressible single phase flows in nuclear engineering applications. *Nucl. Eng. Des.* **2017**, *312*, 2–11. [CrossRef]
5. Xiong, J.; Yang, Y.; Cheng, X. CFD application to hydrogen risk analysis and PAR qualification. *Sci. Technol. Nucl. Install.* **2009**, *2009*, 213981. [CrossRef]
6. Zhou, G.; Yi, X.Y. Development of nuclear power simulation technologies. *Yuanzineng Kexue Jishu/Atomic Energy Sci. Technol.* **2006**, *40*, 23.
7. Reinecke, E.A.; Takenaka, K.; Ono, H.; Kita, T.; Taniguchi, M.; Nishihata, Y.; Hino, R.; Tanaka, H. Performance tests of catalysts for the safe conversion of hydrogen inside the nuclear waste containers in Fukushima Daiichi. *Int. J. Hydrogen Energy* **2021**, *46*, 12511–12521. [CrossRef]
8. Raman, R.K.; Iyer, K.N.; Ravva, S.R. CFD studies of hydrogen mitigation by recombiner using correlations of reaction rates obtained from detailed mechanism. *Nucl. Eng. Des.* **2020**, *360*, 110528. [CrossRef]
9. Yung, T.Y.; Lu, W.F.; Tsai, K.C.; Chuang, C.H.; Chen, P.T. Oxidation Behavior Characterization of Zircaloy-4 Cladding with Different Hydrogen Concentrations at 500–800 °C in an Ambient Atmosphere. *Materials* **2022**, *15*, 2997. [CrossRef]
10. Serrano, C.; Jimenez, G.; Molina, M.d.C.; López-Alonso, E.; Justo, D.; Zuriaga, J.V.; González, M. Proposed methodology for Passive Autocatalytic Recombiner sizing and location for a BWR Mark-III reactor containment building. *Ann. Nucl. Energy* **2016**, *94*, 589–602. [CrossRef]
11. Heitsch, M.; Huhtanen, R.; Téchy, Z.; Fry, C.; Kostka, P.; Niemi, J.; Schramm, B. CFD evaluation of hydrogen risk mitigation measures in a VVER-440/213 containment. *Nucl. Eng. Des.* **2010**, *240*, 385–396. [CrossRef]

12. Matsuda, K.; Tanaka, N.; Majima, H. Dissolution Behavior of Hrdrogen Gas In Aqueous Solutions Containing Strong Electrolytes-2. Studies on The Gaseous Reduction of Metals From Aqueous Solutions. *J Min Metall Inst Jpn.* **1978**, *94*, 1079.
13. Wang, F.; Zhao, M.; Zou, Z.; Deng, J.; Zhang, H.; Zhang, M.; Qin, H. Code Validation and Application of Hy-drogen Mitigation by Passive Autocatalytic Recombiner in Small Modular Reactor. *Nuclear Engineering and Design* **2022**, *396*, 111882. [CrossRef]
14. Hoyes, J.R.; Ivings, M.J. CFD modelling of hydrogen stratification in enclosures: Model validation and application to PAR performance. *Nucl. Eng. Des.* **2016**, *310*, 142–153. [CrossRef]
15. Kelm, S.; Kampili, M.; Liu, X.; George, A.; Schumacher, D.; Druska, C.; Struth, S.; Kuhr, A.; Ramacher, L.; Allelein, H.J.; et al. The tailored CFD package 'containmentFOAM' for analysis of containment atmosphere mixing, H2/CO mitigation and aerosol transport. *Fluids* **2021**, *6*, 100. [CrossRef]
16. Chang, H.J.; Zhao, R.C.; Du, W.F.; Sun, L.L.; Zhou, S.; Wang, Y.Z. Passive containment cooling system thermal-hydraulic test reserch for Chinese large passive nuclear power plant development. In Proceedings of the 17th International Topical Meeting on Nuclear Reactor Thermal Hydraulics, NURETH 2017, Xi'an, China, 3–8 September 2017; Volume 2017.
17. Liu, F.; Sun, Z.; Ding, M.; Bian, H. Research progress of hydrogen behaviors in nuclear power plant containment under severe accident conditions. *Int. J. Hydrogen Energy* **2021**, *46*, 36477–36502. [CrossRef]
18. Ding, P.; Chen, M.; Li, W.; Liu, Y.; Wang, B. CFD simulations in the nuclear containment using the des turbulence models. *Nucl. Eng. Des.* **2015**, *287*, 1–10. [CrossRef]
19. Xiao, J.; Breitung, W.; Kuznetsov, M.; Zhang, H.; Travis, J.R.; Redlinger, R.; Jordan, T. GASFLOW-MPI: A new 3-D parallel all-speed CFD code for turbulent dispersion and combustion simulations: Part I: Models, verification and validation. *Int. J. Hydrogen Energy* **2017**, *42*, 8346–8368. [CrossRef]
20. Chen, Y.H.; Li, T.; Xue, D.L. Research and application of nuclear power plant in-service inspection information management platform. *E3S Web Conf.* **2021**, *257*, 01056. [CrossRef]
21. Jin, S.; Li, X.B.; Gong, J.X. Probabilistic performance evaluation of nuclear containment structure subjected to severe accidents. *Gongcheng Lixue/Engineering Mech.* **2021**, *38*, 103–112. [CrossRef]
22. Gardner, L.; Liang, Z.; Clouthier, T.; MacCoy, R. A large-scale study on the effect of ambient conditions on hydrogen recombiner-induced ignition. *Int. J. Hydrogen Energy* **2021**, *46*, 12594–12604. [CrossRef]
23. Orszulik, M.; Fic, A.; Bury, T. CFD Modeling of Passive Autocatalytic Recombiners. *Nukleonika* **2015**, *60*, 347–353. [CrossRef]
24. Riera, J.E.; Martínez-Val, A.; Muñoz-Cobo, M.A.; Gallego-Marcos, J.M.M.-A. Hydrogen transport in containment buildings during severe accidents: A lumped-parameter model. *Nucl. Eng. Des.* **2014**, 1–10.
25. Hristov, H.V.; Preuß, J.; Buchholz, S.; Schaffrath, A. Validation work for the containment cooling condenser with the system code Athlet within the frame of the German Easy Project. In Proceedings of the 17th International Topical Meeting on Nuclear Reactor Thermal Hydraulics, NURETH 2017, Xi'an, China, 3–8 September 2017; Volume 2017.